Positive impact of indicaxanthin from *Opuntia ficus-indica* fruit on high-fat diet–induced neuronal damage and gut microbiota dysbiosis

Simona Terzo[1], Antonella Amato[1, 2, *], Pasquale Calvi[1, 3], Marta Giardina[1], Domenico Nuzzo[2], Pasquale Picone[2], Antonio Palumbo-Piccionello[1], Sara Amata[1], Ilenia Concetta Giardina[1], Alessandro Massaro[1], Ignazio Restivo[1], Alessandro Attanzio[1], Luisa Tesoriere[1], Mario Allegra[1], Flavia Mulè[1, *]

https://doi.org/10.4103/NRR.NRR-D-23-02039

Date of submission: December 16, 2023

Date of decision: July 26, 2024

Date of acceptance: September 13, 2024

Date of web publication: September 24, 2024

From the Contents

Graphical Abstract

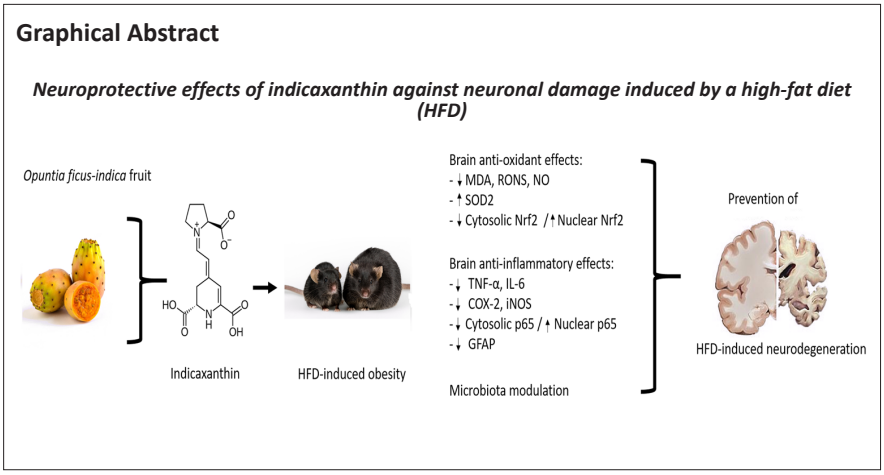

Abstract

Indicaxanthin is a betalain that is abundant in *Opuntia ficus-indica* orange fruit and has antioxidative and anti-inflammatory effects. Nevertheless, very little is known about the neuroprotective potential of indicaxanthin. This study investigated the impact of indicaxanthin on neuronal damage and gut microbiota dysbiosis induced by a high-fat diet in mice. The mice were divided into three groups according to different diets: the negative control group was fed a standard diet; the high-fat diet group was fed a high-fat diet; and the high-fat diet + indicaxanthin group was fed a high-fat diet and received indicaxanthin orally (0.86 mg/kg per day) for 4 weeks. Brain apoptosis, redox status, inflammation, and the gut microbiota composition were compared among the different animal groups. The results demonstrated that indicaxanthin treatment reduced neuronal apoptosis by downregulating the expression of proapoptotic genes and increasing the expression of antiapoptotic genes. Indicaxanthin also markedly decreased the expression of neuroinflammatory proteins and genes and inhibited high-fat diet–induced neuronal oxidative stress by reducing reactive oxygen and nitrogen species, malondialdehyde, and nitric oxide levels. In addition, indicaxanthin treatment improved the microflora composition by increasing the abundance of healthy bacterial genera, known as producers of short-chain fatty acids (*Lachnospiraceae*, *Alloprovetella*, and *Lactobacillus*), and by reducing bacteria related to unhealthy profiles (*Blautia*, *Faecalibaculum*, *Romboutsia* and *Bilophila*). In conclusion, indicaxanthin has a positive effect on high-fat diet–induced neuronal damage and on the gut microbiota composition in obese mice.

Key Words: gut microbiota dysbiosis; high-fat diet; indicaxanthin; microflora; neuronal apoptosis; neurodegeneration; neuroinflammation; obesity; *Opuntia ficus-indica* fruit

Introduction

According to the World Health Organization (WHO), obesity is rapidly increasing worldwide and affects more than 1.12 billion people by 2030 (World Health Organization, 2021). Obesity is caused mainly by a high intake of sugars and fat associated with a sedentary lifestyle and can contribute to various health problems that reduce quality of life and life expectancy, leading to the development of insulin resistance, type 2 diabetes, dyslipidemia, nonalcoholic fatty liver disease and cardiovascular disease. Chronic low-grade inflammation and oxidative stress are linked to these various pathological conditions (Marseglia et al., 2015). Furthermore, obesity affects brain homeostasis, becoming a crucial cause of the development of dementia (O'Brien et al., 2017; Pugazhenthi et al., 2017). Consequently, chronic consumption of a high-fat diet (HFD) is considered a risk factor for cognitive impairment,

[1]Department of Biological- Chemical- Pharmaceutical Science and Technology, University of Palermo, Palermo, Italy; [2]Institute for Biomedical Research and Innovation – IRIB, Palermo, Italy; [3]Department of Biomedicine, Neuroscience and Advanced Diagnostic, University of Palermo, Palermo, Italy
*__Correspondence to:__ Flavia Mulè, flavia.mule@unipa.it; Antonella Amato, antonella.amato@unipa.it.
https://orcid.org/0000-0003-0676-0142 (Flavia Mulè); https://orcid.org/0000-0002-3343-9656 (Antonella Amato)

How to cite this article: *Terzo S, Amato A, Calvi P, Giardina M, Nuzzo D, Picone P, Palumbo-Piccionello A, Amata S, Giardina IC, Massaro A, Restivo I, Attanzio A, Tesoriere L, Allegra M, Mulè F (2025) Positive impact of indicaxanthin from Opuntia ficus-indica fruit on high-fat diet–induced neuronal damage and gut microbiota dysbiosis. Neural Regen Res 20(0):000-000.*

early brain aging and even Alzheimer's disease (AD) (Nuzzo et al., 2015; Snowden et al., 2017; Chudoba et al., 2019; Galizzi et al., 2023). Cerebral damage induced by HFD has been widely characterized in animal models. This process involves neuroinflammation, extensive oxidative stress, alterations of the blood–brain barrier, synaptic loss, central insulin resistance and neuronal cell death (Dinel et al., 2011; Valladolid-Acebes et al., 2011; Nuzzo et al., 2015, 2020; Kim et al., 2016; Wanrooy et al., 2018; Galizzi et al., 2023; Terzo et al., 2023). Several mechanisms have been proposed to link obesity to central nervous system impairment (Picone et al., 2020), including changes in the gut microbiota (Zhang et al., 2019; Shi et al., 2020), but no therapies have been identified yet. Indeed, obese people consuming HFD exhibit gut microbiota dysbiosis associated with worse cognitive ability (Shi et al., 2020), and in rodents, HFD-induced microbiota alterations can impair learning and memory (Zhang et al., 2019). Interestingly, a recent study reported that many cases of dementia may be prevented by addressing diet and lifestyle (Livingston et al., 2020). In particular, a plethora of potential bioactive compounds or food components, such as monoterpene and triterpene polyphenolic compounds, have been reported to possess neuroprotective properties (Habtemariam, 2018; Noori et al., 2021; Wang et al., 2022).

Indicaxanthin (Ind), a phytochemical abundant in the yellow fruits of Opuntia ficus-indica, has been shown to act as an antioxidant in several *in vitro* and *in vivo* experiments (Rahimi et al., 2018; Allegra et al., 2019; Attanzio et al., 2019). Moreover, it exerts anti-inflammatory effects in various models of acute and chronic inflammation, prevents insulin resistance and improves obesity-related glucose dysmetabolism in HFD-fed mice (Allegra et al., 2014; Terzo et al., 2021). Ind is highly bioavailable (Tesoriere et al., 2004) and can cross the blood–brain barrier (Allegra et al., 2015). Nevertheless, very little is known about its neuroprotective potential (Campisi et al., 2021), despite its healthy effects.

In light of the biological activities described above, the purpose of the present study was to evaluate the neuroprotective potential of Ind against the neuronal damage and gut microbiota dysbiosis induced by HFD in animal models.

Methods

Extraction and purification of Ind

Ind was extracted from *Opuntia ficus-indica* fruits (yellow cultivar, San Cono, Sicily, Italy) as detailed in Italian Patent Application No. 102021000015167, filed on 10.06.2021. In brief, fruits were peeled and cut, the pulp was separated from the seeds, and 100 g was homogenized and centrifuged at 3000 × *g* for 10 minutes. The supernatant was recovered, and the pellet was extracted with 100 mL of distilled water and centrifuged as described above. The combined supernatants were subjected to cryodesiccation, and Ind in the resulting aqueous extract was separated by size exclusion chromatography on Sephadex G-25. Fractions containing the pigment were subjected to cryodesiccation, followed by solid-phase extraction on J.T. Baker, Bakerbond SPE C18 columns (VWR, Milan, Italy). The eluate was subjected to rotary evaporation to remove methanol, and the residue was dissolved in phosphate-buffered saline (PBS). The Ind concentration was evaluated via spectrophotometric revelation at 482 nm, with an extinction coefficient of 48/mM/cm. All the samples were aliquoted and stored at –80°C until further use.

Animals and diet

Four-week-old male C57BL/6J (B6) mice (*n* = 24; body weight 18–20 g), purchased from Envigo Laboratories (San Pietro al Natisone, Udine, Italy), were housed in the animal house of the Advanced Technologies Network (ATeN) center under specified environmental conditions (12-hour light/dark cycle, temperature 22–24°C, relative humidity [55 ± 5]%), with free access to water and food.

We chose to use only male mice to avoid hormonal changes linked to the reproductive cycle of the female animals, as previously reported (Terzo et al., 2021). The procedures for the care and use of laboratory animals conformed with European guidelines and were approved by the Ministry of Health (Rome, Italy; Authorization No. 37/2020-PR on 16 January 2020). After 1 week of acclimation, the mice were weighed and randomly divided into two groups, which were fed a standard diet (STD) (70% energy as carbohydrates, 20% protein, and 10% fat; 4RF25, Mucedola, Milan, Italy) (negative control group; *n* = 8) or HFD (*n* = 16) (60% energy as fat, 20% protein, and 20% carbohydrates; PF4051/D, Mucedola) to generate diet-induced obesity. After 10 weeks on HFD, the obese mice were further separated into two subgroups: one group was fed HFD (positive control group; *n* = 8), and the other was fed HFD while receiving Ind orally twice a day (0.4 mg/kg) for 4 weeks (HFD + Ind group, *n* = 8). The mice were assigned to the positive control (HFD) or HFD + Ind group on the basis of body weight to obtain two groups with similar initial conditions before treatment. Ind was administered in water (20 µL). Ind was tested at a nutritionally relevant dose that had previously been demonstrated to prevent glucose impairment and insulin resistance in obese mice (Terzo et al., 2021). At the end of the experimental protocol period, the animals were weighed and sacrificed, and blood was collected via cardiac puncture. The brains were rapidly removed from their skulls, weighed, and cut into two halves coronally. A portion was fixed in 4% formalin for histological assays; the other portion was stored at –80°C for biomolecular analyses. Blood samples were centrifuged at 5,7297 × *g* at 4°C for 15 minutes to obtain plasma, which was stored at –80°C (**Additional Figures 1** and **2**).

Metabolic parameters

The concentrations of triglycerides and cholesterol in blood were determined via a MultiCareIn biochemistry analyzer (Biochemical Systems International, Arezzo, Italy), whereas blood fasting glucose concentrations were determined via a commercial glucometer (GlucoMen LX meter, Menarini, Italy).

Brain tissue preparation

Explanted mouse brains from the STD, HFD, and HFD + Ind groups were coronally divided into two halves. One part was homogenized on ice via a manual Dounce homogenizer

(Omni Internatiomal, Kennesaw, GA, USA), separated into aliquots (5 or 10 mg), immediately transferred to liquid nitrogen and stored at –80°C until analysis (gene expression, immunoblotting, enzyme-linked immunosorbent assay [ELISA], malondialdehyde [MDA] assays, reactive oxygen and nitrogen species [RONS] analyses and nitric oxide [NO] levels). The other part was used for immune-histological assays. Thus, the halves of each brain were fixed in 4% formalin for 24 hours, followed by incubation with graded ethanol (50%, 70%, 85%, and 96%) for 5 minutes each, embedded in paraffin overnight and subsequently sectioned (5 µm thick) via an automatic microtome (Leica Biosystems, Buffalo Grove, IL, USA) (terminal deoxynucleotidyl transferase biotin-dUTP nick end labeling [TUNEL] assay and immunofluorescence).

Terminal deoxynucleotidyl transferase biotin-dUTP nick end labeling assay

Apoptosis was evaluated via the TUNEL assay via a cell death detection kit (Promega, Madison, WI, USA) as previously reported (Nuzzo et al., 2015, 2020; Shi et al., 2020). Briefly, brain samples were cut into 5 µm slices after being embedded in paraffin. Then, the deparaffinized slices were hydrated in a series of graded ethanol solutions (96%, 85%, 70%, and 50%) for 5 minutes each, washed in PBS and incubated with TUNEL working solution for 1 hour at 37°C. Diamidino-2-phenylindole (DAPI) (Invitrogen-Thermo Fisher Scientific, Waltham, MA, USA) solution was used to stain the nucleus. Slices were observed under a fluorescence microscope (Leica Microsystems, Heidelberg, Germany) at a magnification of 20×, and images were collected via the image analysis software Basic Research NIS Elements F 2.30 (Nikon, Florence, Italy). The number of apoptotic nuclei was manually counted by two researchers, who were blinded to the diet type, and the results are expressed in relation to normal nuclei observed in selected fields of the cerebral cortex.

Gene expression

RNA was extracted from the homogenized brain tissue via an RNeasy Mini Kit (Qiagen, Valencia, CA, USA) according to the manufacturer's instructions. A high-capacity cDNA reverse transcription kit (Applied Biosystems, Waltham, MA, USA) was subsequently used to reverse transcribe 2 ng of total RNA into cDNA. Only high-quality RNA samples were used for the experiments.

Semiquantitative polymerase chain reaction experiments

Semiquantitative polymerase chain reaction (PCR) experiments were performed to evaluate the expression of proapoptotic and antiapoptotic genes (*Fas-L*, *Bim*, *P27*, *Bcl-2*, and brain-derived neurotrophic factor [*BDNF*]). The primer sequences are listed in **Table 1**. Semiquantitative gene expression was evaluated by densitometry. The band intensities of the specific amplicons were obtained via ImageJ software (version 1.53f, Laboratory for Optical and Computational Instrumentation-LOCI, University of Wisconsin, USA) and normalized to the corresponding *β-actin* mRNA expression. The expression levels of the mRNAs are represented as the ratio of the mean optical density of the mRNA to that of *β-actin* and are shown as arbitrary units.

Table 1 | **Semiquantitative polymerase chain reaction primer sequences for various genes**

Gene	Forward primer (5'–3')	Reverse primer (5'–3')	Size (bp)
Fas-L	5′-AGC AGT CAG CGT CAG AGT TC-3′	5′-GTA CTG GGG TTG GCT CAC G-3′	442
Bim	5′-GGA GGA GGC GGA GGA TGA T-3′	5′-TCC TGT CTT GCG GTT CTG TC-3′	366
P27	5′-AGA TAC GAG TGG CAG GAG GT-3′	5′-TGT TTA CGT CTG GCG TCG AA-3′	381
Bcl-2	5′-ATG TGT GTG GAG AGC GTC AA-3′	5′- AGA GAC AGC CAG GAG AAA TCA-3′	182
BDNF	5′-GGC TGA CAC TTT TGA GCA CGT C-3′	5′-CTC CAA AGG CAC TTG ACT GCT G-3′	133
β-actin	5′-CGG GAT CCC CGC CCT AGG CAC CAG GGT-3′	5′-GGA ATT CGG CTG GGG TGT TGA AGG TCT CAA A-3′	301

Real-time PCR assays

Real-time PCR (qPCR) was performed to evaluate the expression of inducible nitric oxide synthase (*iNOS*), tumor necrosis factor-α (*TNF-α*) and interleukin (*IL-6*) genes in the brains of the mice. cDNA was amplified via RT2 SYBR Green/ROX qPCR Mastermix (Qiagen) and a StepOne Real-Time instrument (Applied Biosystems). The primer sequences are listed in **Table 2**. Real-time PCR experiments were performed in compliance with the minimum information for publication of quantitative real-time PCR experiments (MIQE) guidelines (Bustin et al., 2009). The amplification efficiencies for all the genes analyzed ranged from 88% to 102%. Gene-specific amplification was confirmed by a single peak in the melting curve analysis and a single band of the expected size on a 2% agarose gel stained with SYBR™ Green nucleic acid gel stain. The average standard deviation of all the samples studied was 0.10 cycles. Relative mRNA expression was calculated via the $2^{-\Delta\Delta Ct}$ approximation method via SDS software (Applied Biosystems). The expression of the *β-actin* gene was also quantified in a similar way for normalization. The expression levels of mRNAs are indicated as the fold change.

Table 2 | **Quantitative polymerase chain reaction primer sequences for various genes**

Gene	Forward primer (5'–3')	Reverse primer (5'–3')	Size (bp)
iNOS	5′-GCA GAA TGT GAC CAT CAT GG-3′	5′-ACA ACC TTG GTG TTG AAG GC-3′	503
TNF-α	5′-GCC CAC GTC GTA GCA AAC CAC-3′	5′-GGC TGG CAC CAC TAG TTG GTT GT-3′	260
IL-6	5′-TCC AGT TGC CTT CTT GGG AC-3′	5′-GTG TAA TTA AGC CTC CGA CTT G-3′	600
β-actin	5′-CGG GAT CCC CGC CCT AGG CAC CAG GGT-3′	5′-GGA ATT CGG CTG GGG TGT TGA AGG TCT CAA A-3′	301

Western blot analysis

Protein quantification from homogenate brain tissue was performed via Bradford assays. Fifty micrograms of protein sample was resolved via SDS-PAGE (Sigma-Aldrich, St. Louis, MO, USA) on 8% acrylamide gels and blotted onto nitrocellulose membranes (Thermo Fisher Scientific, Monza, Italy). After blocking for 2 hours in 5% (w/v) skim milk, the membranes were incubated overnight at 4°C in the presence

of the primary antibodies shown in **Table 3** (1:1000 dilution, Santa Cruz Biotechnology, Milan, Italy). The membranes were then incubated for 90 minutes at room temperature with goat anti-mouse IgG and HRP-conjugated secondary antibodies (1:10,000 dilution; Merck, Milan, Italy; Cat# 12--349; RRID: AB_390192). Specific chemiluminescent bands were detected via a C-Digit Blot Scanner (LI-COR, Lincoln, NE, USA), and densitometry was performed via LI-COR Image Studio 4.0 (LI-COR). Protein expression levels were normalized to those of β-actin and laminin β.

Table 3 | **Primary antibodies used for Western blot analysis**

Protein	Cat#	Host organism	RRID	Clone	Molecular weight (kDa)
COX-2	sc-376861	Mouse	AB_2722522.	H-3	72/70
iNOS	sc-7271	Mouse	AB_627810	C-11	130
p65	sc-8008	Mouse	AB_628017	F-6	65
SOD-2	sc-137254	Mouse	AB_2191808	E-10	25
Nrf-2	sc-365949	Mouse	AB_10917561	A-10	61
Insulin Rβ	sc-57342	Mouse	AB_784102	CT-3	95
β-actin	sc-47778	Mouse	AB_626632	C-4	43
Lamin B	sc-365962	Mouse	AB_10848566	C-5	67

COX-2: Cyclooxygenase-2; iNOS: inducible nitric oxide synthase; SOD-2: superoxide dismutase-2.

Enzyme-linked immunosorbent assay

TNF-α and IL-1β levels in mouse plasma were measured via commercially available ELISA kits (Life Technologies, Frederick, MD, USA); plasma insulin levels were quantified via an ELISA kit (Mercodia, Uppsala, Sweden) and calculated via a plate reader system (Synergy HT microplate reader, Biotech, Winooski, VT, USA).

Immunofluorescence

Portions of the brains removed from the mice were fixed in 4% formalin for 24 hours and embedded in paraffin. Coronal sections (5 μm) were mounted on slides and deparaffinized using xylene solution. Next, the sections were incubated with a mouse primary antibody against glial fibrillary acidic protein (GFAP) (1:300, Cell Signaling Technology, Danvers, MA, USA, Cat# 3670, RRID: AB_10693476) at 4°C overnight and then with an anti-mouse IgG-Alexa Fluor 594 secondary antibody (goat, 1:300, Invitrogen, Cat# A-11005, RRID: AB_2534073) for 2 hours at room temperature. Nuclear staining was performed via Hoechst 33258, and the samples were visualized with a Leica DM4000 microscope (Leica Microsystems) at a magnification of 10×. Negative controls were generated by omitting the primary antibodies. GFAP marker expression was calculated as the percentage of cells that were doubly positive for Hoechst and GFAP compared with the total number of Hoechst-positive cells.

Malondialdehyde assay

MDA levels were assessed in homogenized tissue obtained from coronal portions of mouse brains according to a previously reported method (Allegra et al., 2015). Briefly, a mixture containing 0.2 mL of homogenate, 0.2 mL of 8.1% SDS, 1.5 mL of acetic acid solution at pH 3.5 with NaOH, and 1.5 mL of 1% TBA aqueous solution was prepared, increased to 4.0 mL with distilled water and heated at 95°C for 60 minutes. After the solution cooled, 1.0 mL of distilled water and 5.0 mL of an n-butanol/pyridine solution (15/1, v/v) were added. The mixture was shaken vigorously and then centrifuged at 14,668 × *g* for 10 minutes. The absorbance of the organic layer was evaluated at 532 nm, and the MDA levels were expressed as nmol MDA/g tissue, with 1,1,3,3-tetramethoxypropane used as an external standard. Measurements were performed via a microplate reader (LTek, INNO, Seongnam, South Korea).

Analysis of reactive oxygen and nitrogen species

To evaluate the RONS levels, 50 mg of brain tissue was homogenized with 500 μL of cold PBS and 10 μL of protease inhibitors (Amersham Life Science, Munich, Germany) and then centrifuged at 1123 × *g* for 5 minutes at 4°C. The supernatant was incubated with 10 μM dichlorofluorescein diacetate (DCFH-DA) (Sigma–Aldrich, Milan, Italy) in the dark at 37°C for 30 minutes, after which the fluorescence was evaluated with a fluorimeter (GloMax® Plate Reader, Promega) with an excitation filter at 490 nm and an emission filter at 540 nm.

Determination of nitric oxide levels

The levels of NO in brain tissue were assessed via the Griess reagent. Briefly, 50 mg of brain tissue was homogenized with 500 μl of cold PBS and centrifuged at 1123 × *g* for 5 minutes at 4°C. Afterward, 100 μL of the supernatant was mixed with 100 μL of Griess reagent (equal volumes of 1% sulphanilamide (w/v) in 5% phosphoric acid (v/v) and 0.1% naphthylenediamine-HCl (w/v)) and incubated at room temperature for 10 minutes. The absorbance was then evaluated at 550 nm via a microplate reader (LTek, INNO). Nitrite levels in the samples were evaluated by referring to a standard sodium nitrite serial dilution curve.

Gut microbiota composition

Fecal samples were collected from individual mice in autoclaved tubes and stored at –80°C. A DNA isolation kit (QIAamp DNA StoolHandbook Kit, Qiagen) was used to extract DNA (eight replicates in each dietary group) following the manufacturer's instructions. The extracted DNA was used for the metagenomic study carried out by the BMR Genomics Company (Padova, Italy). For NGS, PCR was performed with modified primers (Pro341F/Pro805R) (Takahashi et al., 2014) targeting the V3–V4 regions of microbial ribosomal RNA genes (small subunits), following the standard protocol of targeted amplicon sequencing. PCR amplification was performed in a final volume of 25 μL via Taq Platinum HiFi (Thermo Fisher Scientific) at 94°C for 1 minute, followed by 25 cycles of 94°C for 30 seconds, 55°C for 30 seconds, and 68°C for 45 seconds. After that, the PCR products were purified via Agencourt XP 1X magnetic beads (Thermo Fisher Scientific) and processed directly into the preparation of sequencing libraries via the Illumina MiSeq platform (San Diego, CA, USA). The UCLUST algorithm (Qime 2) was used for taxonomic annotations for seeds and unmatched nonseed sequences to obtain a minimum threshold of 97% against the Greengenes v13.8 database (Qime 2) (https://docs.qiime2.org/2022.2/

data-resources/). Operational taxonomic units (OTUs) were collected from the biom file and filtered at 0.005% abundance to eliminate spurious OTUs that were present at a low frequency.

Determination of short-chain fatty acids in plasma

Short-chain fatty acids (SCFAs) were evaluated in the plasma samples of the different animal groups via derivatization with 1-(3-dimethylaminopropyl)-3-ethylcarbodiimide hydrochloride (EDC) and 3-nitrophenylhydrazine (3-NPH) and determined via reversed-phase high-performance liquid chromatography coupled with mass spectrometry with electron spray ionization and a triple-quadrupole time-of-flight detector (HPLC/MS/ESI/Q-TOF) (Agilent Technologies Inc., Santa Clara, CA, USA), adapting a previously reported method (Jardou et al., 2021).

Statistical analysis

No statistical methods were used to predetermine sample sizes; however, our sample sizes are similar to those reported in previous publications (Terzo et al., 2021). The results are presented as the mean ± SEM, and the n values represent the number of samples. The data were analyzed via GraphPad Prism 6 software (Graph Pad software, San Diego, CA, USA). Statistical significance was evaluated by analysis of variance followed by the Bonferroni *post hoc* comparison test. Permutational multivariate analysis of variance (PERMANOVA) was used to analyze beta diversity among the different groups of animals. A P value < 0.05 was considered statistically significant.

Results

Metabolic parameters

Compared with those of STD mice, the body weights, plasma fasting glucose and insulin concentrations, HOMA indices, cholesterol and triglyceride levels, and liver and fat masses of HFD-fed mice were significantly greater (**Figure 1A–L**). These observations suggest that 14-week HFD leads to the development of obesity, with dysregulation of glucose and lipid metabolism and the onset of insulin resistance.

In accordance with previously reported results (Terzo et al., 2021), Ind supplementation significantly and selectively improved weight gain, fat mass and glucose dysmetabolism, counteracting peripheral insulin resistance (**Figure 1A–E** and **1I**). Moreover, Western blot analysis revealed that insulin receptor expression in HFD-fed brains was significantly lower (P < 0.001) than that in STD-fed brains, suggesting the presence of central insulin resistance. This downregulation was not evident in the HFD + Ind brains, as their insulin receptor expression was similar to that in the STD brain (**Figure 1F** and **G**), suggesting a positive impact of Ind on central insulin resistance.

Ind prevents neuronal apoptosis in the cerebral cortex of high-fat diet-fed mice

The presence of neuroapoptosis was evaluated in superficial cortex sections via a TUNEL assay, which can reveal fragmented DNA, indices of cell death, and comparative analyses of the gene expression of proapoptotic and antiapoptotic factors. Compared with STD animals, HFD-fed brains presented a significant increase in the number of apoptotic neurons; strong gene overexpression of the proapoptotic proteins *Fas-L*, *Bim*, and *P27*; and a significant reduction in the expression of the antiapoptotic proteins *Bcl-2* and *BDNF* (**Figure 2A–F**). Moreover, we observed significantly fewer apoptotic cells in Ind-treated mice than in HFD-fed mice (P < 0.001; **Figure 2A** and **B**). Furthermore, the HFD-induced gene upregulation of the proapoptotic proteins *Fas-L* (P < 0.01), *Bim* (P < 0.05), and *P27* (P < 0.01) was significantly attenuated by Ind treatment compared with that of the HFD-fed group (**Figure 2C** and **D**). Accordingly, the gene expression of the antiapoptotic proteins *Bcl-2* and *BDNF* was similar to that of STD mice in the HFD + Ind group (**Figure 2E** and **F**), suggesting that Ind was able to prevent HFD-induced neuroapoptosis.

Ind mitigates brain oxidative damage induced by a high-fat diet

Oxidative stress plays a crucial role in brain damage, including obesity-related neurodegenerative pathologies (Anjum et al., 2018). Consequently, we evaluated the impact of Ind on oxidative stress in the brain. As shown in **Figure 3A–C**, the MDA levels, lipid peroxidation indices, RONS and NO levels were significantly greater in HFD-fed brains than in STD-fed brains (P < 0.001) but were not elevated in the brains of Ind-treated mice. In addition, Western blot analysis revealed that the expression of the antioxidant enzyme superoxide dismutase (SOD-2) was significantly lower (P < 0.001) in HFD-fed brains than in STD-fed and HFD + Ind-fed brains (**Figure 3D** and **E**).

In light of the key role of Nrf-2 in the maintenance of intracellular redox homeostasis, we next evaluated Nrf-2 activation (assessed as its nuclear translocation) in the brains of the different groups of mice. We detected reduced nuclear accumulation of Nrf-2 in HFD-fed brains than in STD-fed brains (P < 0.001). In addition, HFD + Ind brains presented greater Nrf-2 nuclear accumulation that HFD-fed brains (P < 0.001), suggesting a key role for this transcription factor in the antioxidative activity of Ind (**Figure 3F** and **G**). These results suggest that Ind is able to ameliorate the oxidative stress induced by HFD in the brain, probably through the Nrf-2 pathway.

Ind ameliorates high-fat diet-induced brain inflammation

Oxidative stress and inflammation are mutually linked and are closely associated with neurodegeneration (Kempuraj et al., 2016). Consequently, we evaluated whether and how Ind treatment could alleviate HFD-induced neuroinflammation. Molecular analyses of proinflammatory parameters revealed that the gene upregulation of *iNOS*, *TNF-α*, and *IL-6* observed in HFD-fed brains was significantly decreased in HFD + Ind-fed brains (P < 0.001), as was the protein overexpression of iNOS and cyclooxygenase-2 (COX-2) (P < 0.001; **Figure 4A–C**). Moreover, the nuclear translocation of NF-kB, a key transcription factor involved in the elaboration of proinflammatory mediators, was increased in HFD-fed brains. Notably, these effects were mitigated by Ind treatment (**Figure 4D** and **E**).

Furthermore, to confirm the anti-inflammatory activity of Ind in the brain, the presence of GFAP, an index of astrocyte activation and gliosis in the brain, was evaluated in brain sections from different animal groups via

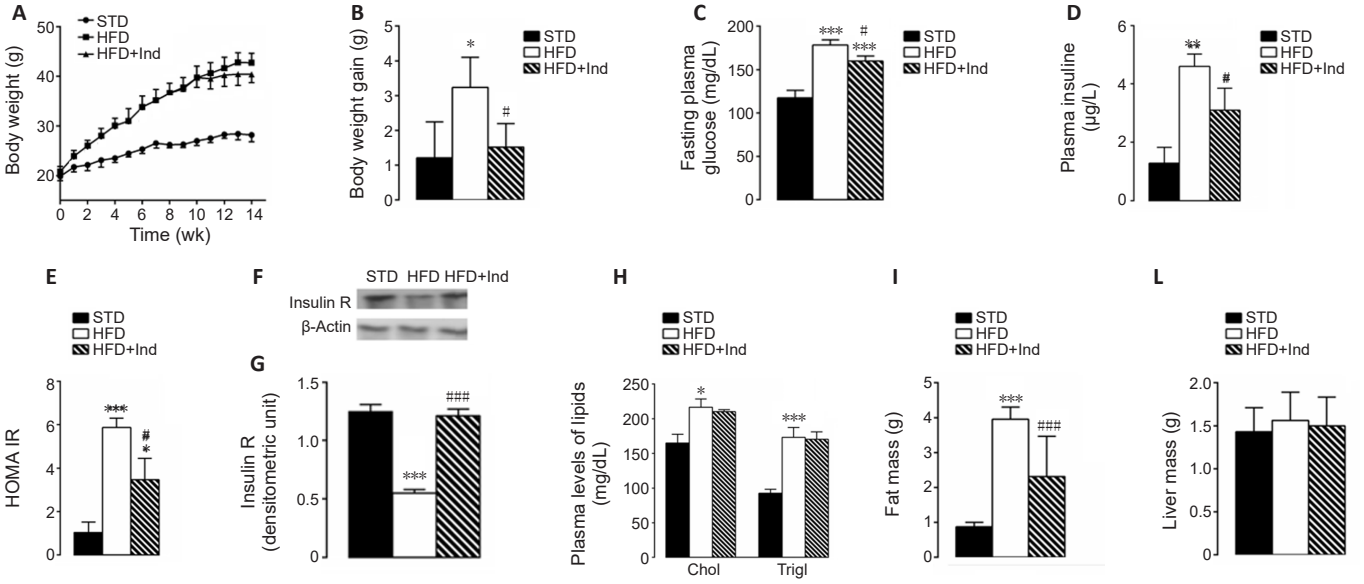

Figure 1 | **Metabolic parameters of the different groups of mice.**
(A) Body weight during the study period. (B) Final body weight gain. (C) Fasting blood glucose concentration. (D) Fasting insulin concentration. (E) The HOMA index was calculated as fasting glucose (mg/dL) × fasting insulin (ng/mL)/22.5. (F) Brain insulin receptor expression. (G) Densitometric analysis of insulin R protein levels normalized to β-actin levels in STD, HFD, and HFD + Ind mice. (H) Plasma levels of cholesterol and triglycerides. (I) Fat mass. (L) Liver mass. Data are presented as the mean ± SEM (n = 8/group). *P < 0.05, **P < 0.01, ***P < 0.001, *vs*. STD mice; #P < 0.05, ###P < 0.001, *vs*. HFD-fed mice. Chol: cholesterol; HFD: high-fat diet; Ind: indicaxanthin; STD: standard diet; Trigl: triglycerides.

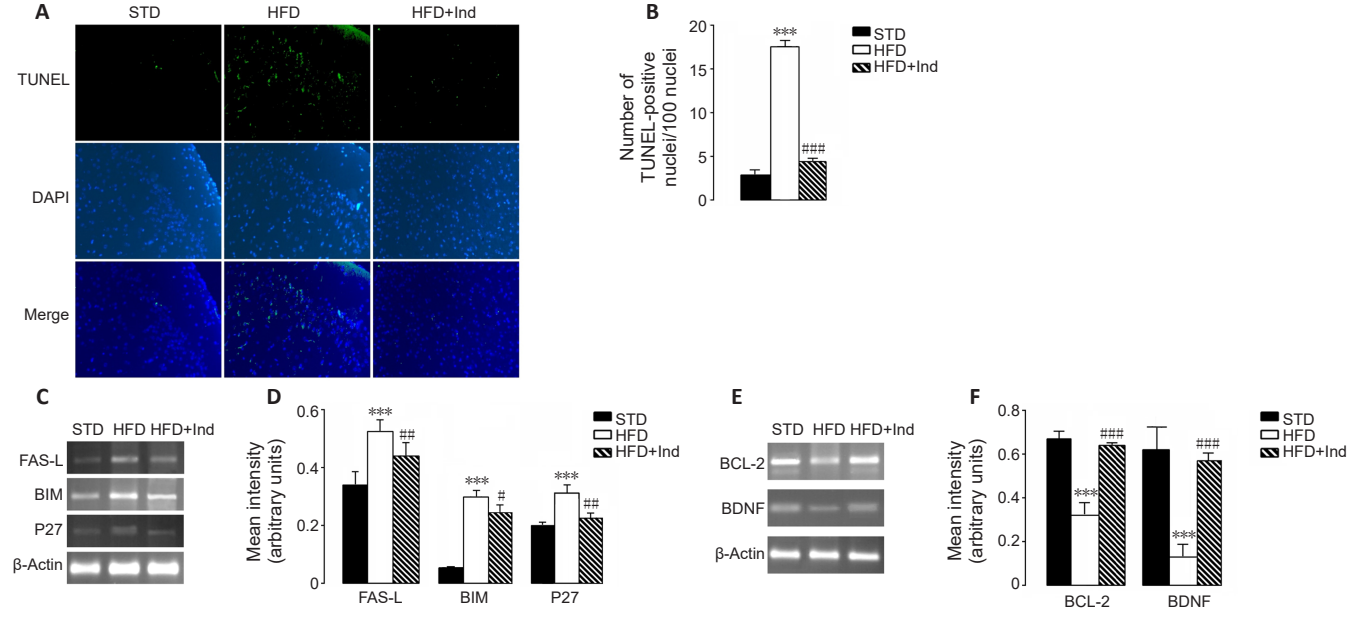

Figure 2 | **Indicaxanthin prevents HFD-induced neuronal apoptosis.**
(A) TUNEL assay in the superficial cerebral cortex (microscope magnification 20×), showing blue (DAPI-stained nuclei) and red (TUNEL-positive cells) staining. Scale bars: 200 µm. (B) Number of apoptotic nuclei in the superficial cerebral cortex. (C) Results of semiquantitative PCR and (D) mRNA levels of the proapoptotic genes Fas-L, Bim, and P27 in the mouse brain. (E, F) Representative image of the semiquantitative PCR results (E) and mRNA levels of the survival genes *Bcl-2* and *BDNF* (F) in the mouse brain. Data are presented as the mean ± SEM (n = 8/group). ***P < 0.001, *vs*. STD mice; #P < 0.05, ##P < 0.01; ###P < 0.001, *vs*. HFD-fed mice. BDNF: Brain-derived neurotrophic factor; HFD: high-fat diet; Ind: indicaxanthin; PCR: polymerase chain reaction; STD: standard diet; TUNEL: terminal deoxynucleotidyl transferase biotin-dUTP nick end labeling.

immunofluorescence. The analysis revealed increased GFAP immunoreactivity in the superficial cerebral cortex of HFD-fed animals compared with that in STD-fed animals (P < 0.001). This increase was not observed in HFD + Ind mice. In fact, the number of GFAP-positive cells in the cerebral sections from HFD + Ind mice was similar to that in the STD-mice (**Figure 4F** and **G**). However, the plasma concentrations of the inflammatory cytokines TNF-α and IL-1β, which were significantly greater in HFD-fed mice than in STD-fed mice (P < 0.001), were not significantly modified by Ind treatment (**Figure 4H** and **I**). These results suggest that Ind is able to mitigate HFD-induced neuroinflammation.

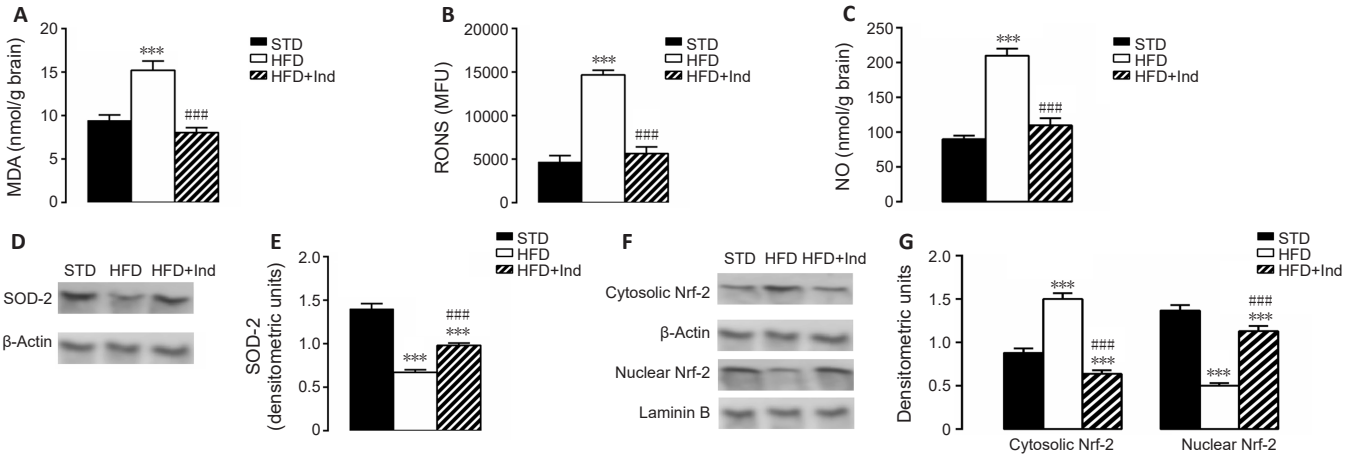

Figure 3 | **Indicaxanthin mitigates brain oxidative damage induced by HFD.**
(A–D) Levels of cerebral MDA (A), RONS (B), and NO(C), and SOD-2 protein expression (D). (E) Densitometric analysis of SOD-2 protein levels normalized to β-actin levels. (F) Brain expression of cytosolic and nuclear Nrf-2. (G) Densitometric analysis of cytosolic Nrf-2 protein levels normalized to β-actin levels and nuclear Nrf2 normalized to laminin B levels. Data are presented as the mean ± SEM (n = 8/group). ***P < 0.001, *vs*. STD mice; ###P < 0.001, *vs*. HFD-fed mice. HFD: High-fat diet; Ind: indicaxanthin; MDA: malondialdehyde; NO: nitric oxide; RONS: reactive oxygen and nitrogen species; SOD-2: enzyme superoxide dismutase-2; STD: standard diet; TUNEL: terminal deoxynucleotidyl transferase biotin-dUTP nick end labeling.

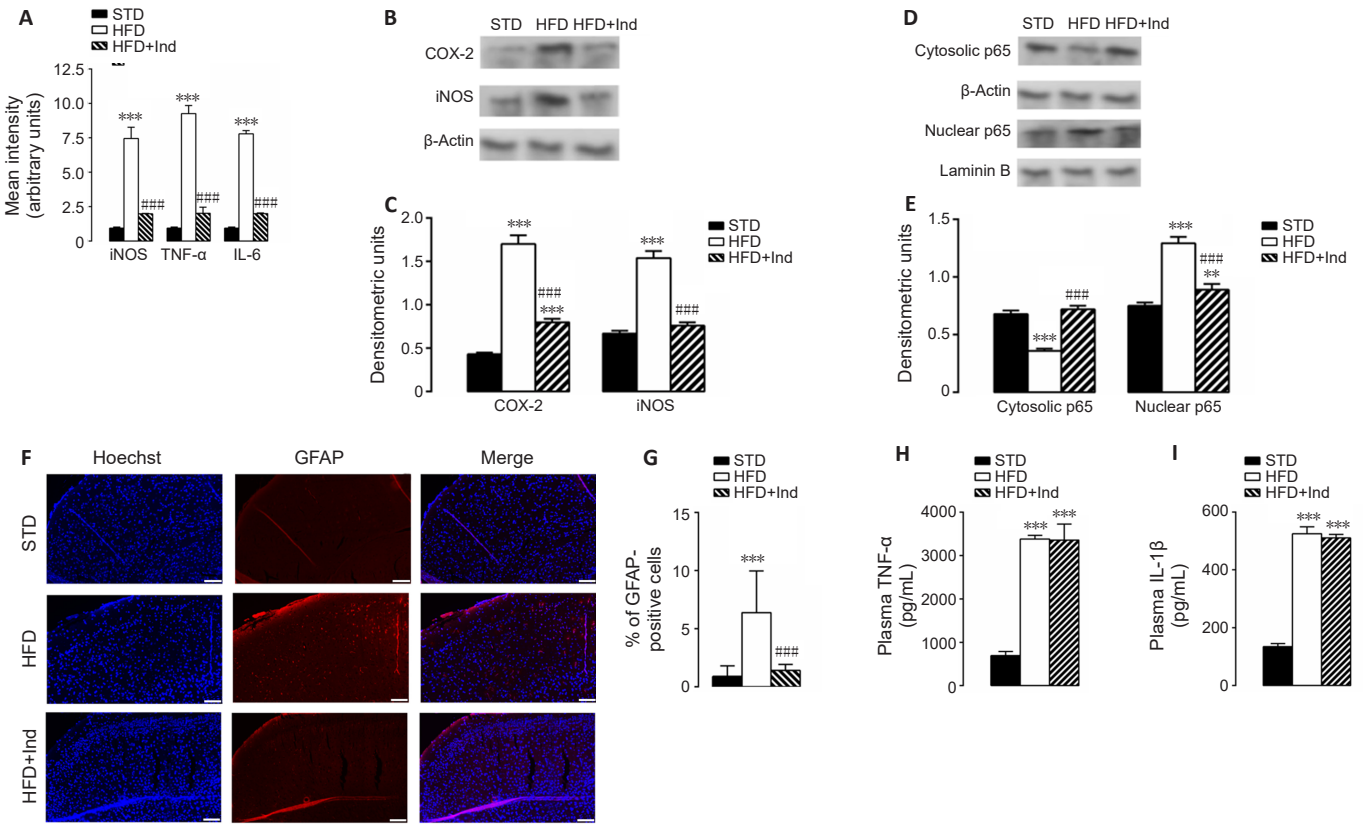

Figure 4 | **Indicaxanthin ameliorates brain inflammation induced by HFD.**
(A) Transcription levels of iNOS, TNF-α, and IL-6 determined by quantitative real-time PCR in the brain. (B) Brain expression of COX-2 and iNOS. (C) Densitometric analysis of COX-2 and iNOS protein levels normalized to β-actin levels. (D) Brain expression of cytosolic and nuclear p65. (E) Densitometric analysis of cytosolic p65 protein levels normalized to β-actin levels and nuclear p65 levels normalized to laminin B levels. (F) Representative images of GFAP-positive cells (red) on the surface. Hoechst staining was used to label the nuclei (blue) (microscope magnification 10×); scale bars: 100 μm. (G) Percentage of GFAP-positive cells; (H, I) Plasma circulating levels of TNF-α (H) and IL-1β (I). Data are presented as the mean ± SEM (n = 8/group). ***P < 0.001, *vs*. STD mice; ###P < 0.001, *vs.* HFD-fed mice. COX-2: Cyclooxygenase-2; GFAP: glial fibrillary acidic protein; HFD: high-fat diet; IL-6: interleukin-6; Ind: indicaxanthin; iNOS: inducible nitric oxide synthase; PCR: polymerase chain reaction; STD: standard diet; TNF-α: tumor necrosis factor-α.

Ind modulates the gut microbiota in high–fat diet-fed mice

Changes in the gut microbiota have been associated with neuroinflammatory, neurodegenerative and psychiatric disorders, leading to the hypothesis that modulation of the gut microbiota may prevent or improve the development and progression of CNS pathologies (Fung et al., 2017). Therefore, we examined whether Ind affects the diversity and composition of the gut microbiota in HFD-fed mice via next-generation sequencing (NGS) analysis. Compared with those of STD mice, the α diversity indices of HFD-fed mice (observed features, Shannon entropy and Pielou evenness) were significantly lower ($P < 0.05$), but no difference was observed in comparison with those of the HFD + Ind group (**Figure 5A–C**). β-Diversity analysis revealed that the HFD group was different from the STD group ($P < 0.001$) but similar to the HFD + Ind group (**Figure 5D** and **E**).

At the phylum level, HFD ($P < 0.01$) and HFD + Ind ($P < 0.05$) mice presented a significant reduction in the abundance of *Bacteroidetes* and an increase in *Firmicutes* ($P < 0.01$) and, consequently, in the *Firmicutes*/*Bacteroidetes* ratio in comparison to STD mice ($P < 0.001$; **Figure 6A** and **B**). In terms of the relative abundance of the other minor phyla, we found a significant reduction in *Desulfobacterota* ($P < 0.05$), *Proteocacteria* ($P < 0.001$) and *Deferribacterota* ($P < 0.001$) in the HFD + Ind group; however, these bacteria were increased in HFD-fed mice (**Figure 6C**).

At the family level, the HFD-fed group presented decreased *Lactobacillaceae* ($P < 0.05$) and *Prevotella* ($P < 0.001$) and increased *Erysipelotrichaceae* and *Deferribacteraceae* ($P < 0.01$) in comparison with the STD-fed group, whereas Ind supplementation mainly increased *Lactobacillaceae* ($P < 0.01$) and *Prevotellaceae* ($P < 0.01$) and significantly decreased *Erysipelotrichaceae* ($P < 0.001$) and *Deferrobacter* ($P < 0.001$) in comparison with the HFD-fed group (**Figure 7A**). Intriguingly, Ind treatment also increased *Lachnospiraceae_NK4A136*, *Lactobacillus*, and *Alloprevotella* but reduced *Blautia*, *Faecalibaculum*, *Mucispirillum*, *Bilophila*, and *Candiatus Saccharimonas* at the genus level, with increased *Bacteroides vulgatus* and *Lactobacillus johnsonii* and a decrease in *Clostridium* at the species level, suggesting that Ind could positively modulate HFD-induced changes in the gut microbiota (**Figure 7B** and **C**).

Finally, we analyzed SCFA levels, namely, acetate, propionate and butyrate, in the plasma of different mice using HPLC/MS. We found that HFD decreased acetate, whereas Ind supplementation increased plasma acetate (**Figure 7D**). The propionate and butyrate concentrations were under the limit of detection (0.5 μM) in all the cases.

Discussion

In the present study, we show, for the first time, a large range of beneficial effects of Ind, which is extracted from the yellow cultivar *Opuntia ficus-indica* fruit, on HFD-induced brain neuronal damage in mice. In particular, Ind treatment, at a nutritionally relevant dose, was able to prevent neurodegeneration, improve brain oxidative stress and neuroinflammation and positively modulate the composition and abundance of some bacterial phyla, families, genera and species in the gut.

Obesity is a key risk factor for the development of neurodegenerative diseases and cognitive impairments (Miller and Spencer, 2014; O'Brien et al., 2017). Epidemiological studies have demonstrated that obese people who consume a high proportion of saturated fats exhibit a dysmetabolism-related reduction in cognitive ability (Morris et al., 2004). Accordingly, in rodents, HFD induces neurodegeneration, impaired spatial learning and significant behavioral deficits (Dinel et al., 2011; Valladolid-Acebes et al., 2011).

Our results clearly show that chronic HFD intake leads to obesity, hyperglycemia, dyslipidemia and peripheral insulin resistance, in accordance with previous data (Kim et al., 2016; Nuzzo et al., 2020; Terzo et al., 2021, 2023), along with neuropathologies characterized by central insulin resistance, neuroapoptosis, oxidative stress and neuroinflammation. Treatment with Ind positively impacted metabolic and

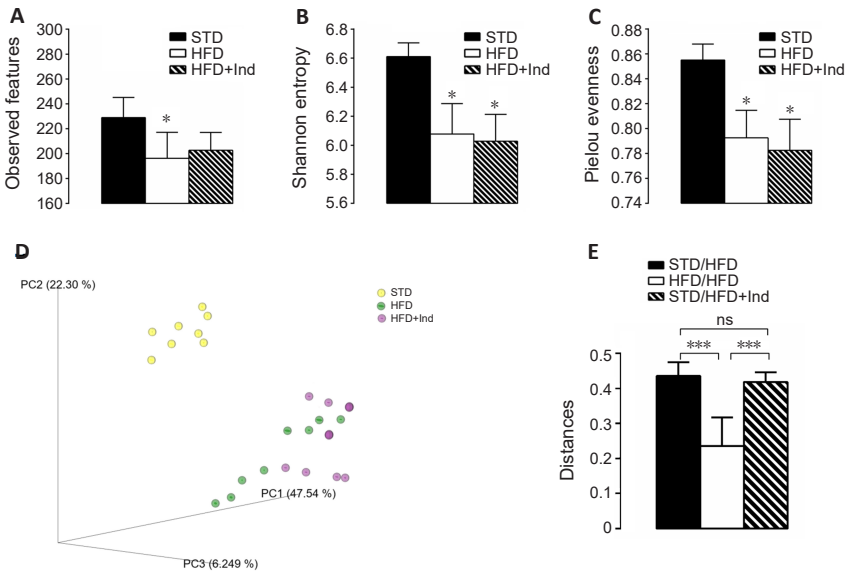

Figure 5 | Gut bacterial diversity in the different animal groups.、
(A–C) Alpha diversity of the gut microbiota on the basis of average observed features (A), average Shannon entropy (B), and average Pielou evenness (C). Beta diversity (unweighted UniFrac) of the gut microbiota in STD, HFD, and HFD + Ind animals: (D) principal coordinate (PC) analysis of each fecal sample bacterial profile analyzed in the different animal groups; (E) statistical comparison of beta diversity among the STD, HFD, and HFD + Ind group (permutational multivariate analysis of variance). Data are presented as the mean ± SEM (n = 8/group). *$P < 0.05$, *vs*. STD mice; ***$P < 0.001$, *vs*. HFD-Ind mice. HFD: High-fat diet; Ind: indicaxanthin; ns: not significant; STD: standard diet.

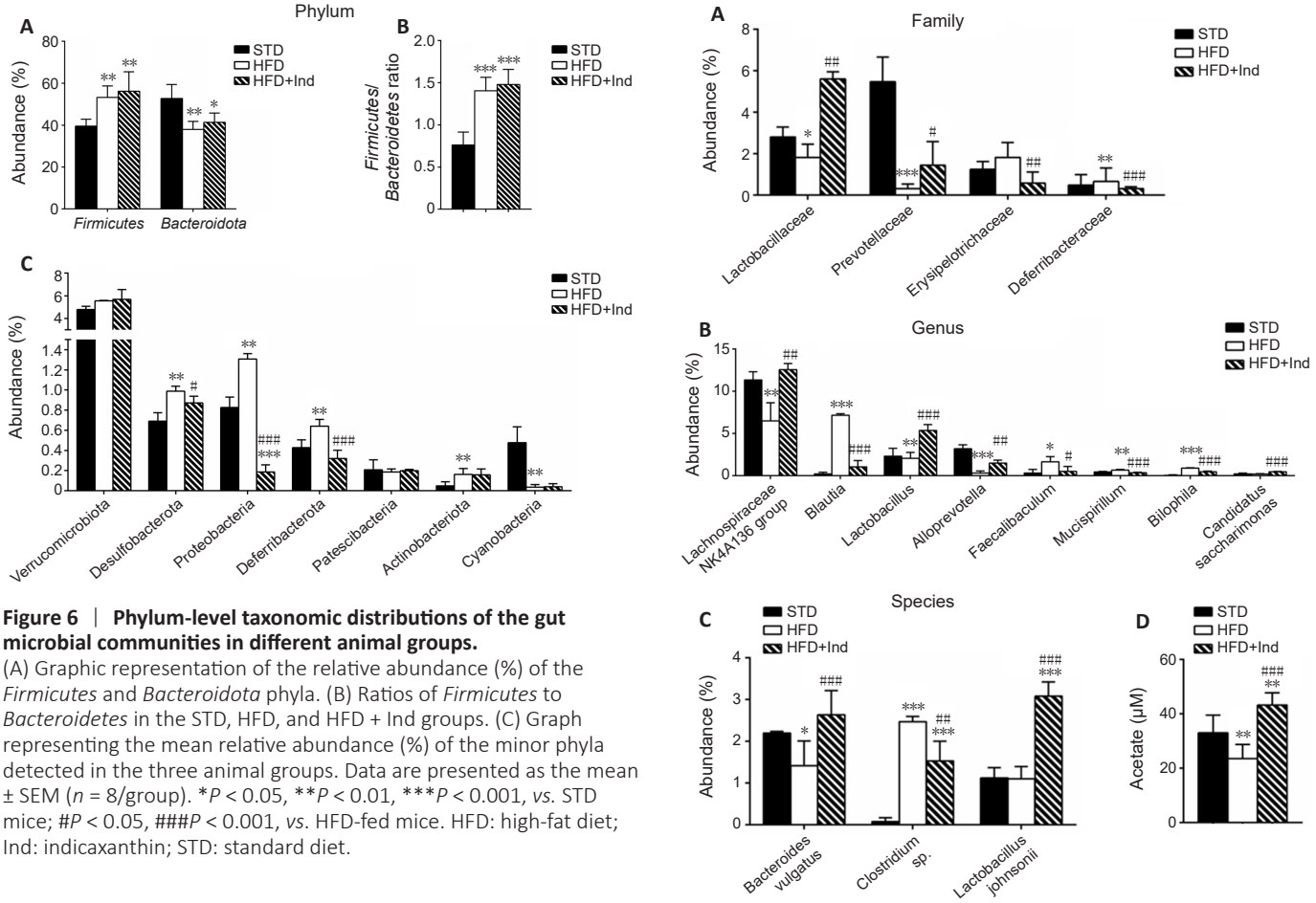

Figure 6 | Phylum-level taxonomic distributions of the gut microbial communities in different animal groups.
(A) Graphic representation of the relative abundance (%) of the *Firmicutes* and *Bacteroidota* phyla. (B) Ratios of *Firmicutes* to *Bacteroidetes* in the STD, HFD, and HFD + Ind groups. (C) Graph representing the mean relative abundance (%) of the minor phyla detected in the three animal groups. Data are presented as the mean ± SEM (n = 8/group). *P < 0.05, **P < 0.01, ***P < 0.001, *vs.* STD mice; #P < 0.05, ###P < 0.001, *vs*. HFD-fed mice. HFD: high-fat diet; Ind: indicaxanthin; STD: standard diet.

Figure 7 | Taxonomic distributions of the gut microbial communities in the different animal groups at the family, genus, and species levels.
(A–C) Family (A), genus (B), and species abundance (C) significantly modified by indicaxanthin treatment. (D) Analysis of the plasma acetate concentration in the STD, HFD, and HFD + Ind groups. Data are presented as the mean ± SEM (n = 8/group). *P < 0.05, **P < 0.01, ***P < 0.001, *vs*. STD mice; #P < 0.05, ##P < 0.01, ###P < 0.001, *vs*. HFD-fed mice. HFD: High-fat diet; Ind: indicaxanthin; STD: standard diet.

neurodegenerative parameters. In particular, it reestablished brain insulin receptor expression, suggesting that this phytochemical has the ability to ameliorate insulin functions in the brain.

Because dysregulated apoptosis has been implicated in the pathogenesis of neurodegenerative disorders (Jaiswal and Sharma, 2017), we examined the effects of Ind on programmed neuronal death. Compared with that in the STD cortex, the number of TUNEL-positive neurons, which was significantly greater in the HFD cortex, was lower in the cortex of HFD + Ind animals, demonstrating the ability of Ind to exert significant neuroprotective effects. Furthermore, we evaluated the expression of several pro- and antiapoptotic genes, including *Bim*, *Fas-L*, *P27*, *Bcl-2* and *BDNF*, in the different animal groups. Bim belongs to the BH3-only protein family and promotes apoptosis by activating Bax (Maes et al., 2017). Fas-L has previously been reported to mediate apoptosis in neurodegenerative disorders (Ethell and Buhler, 2003). *P27*, an inhibitor of cyclin-dependent kinases, injures neurons under neurotoxic conditions by promoting apoptosis (Jaiswal and Sharma, 2017). *Bcl-2*, an antiapoptotic factor, enhances cell survival in response to diverse apoptotic stimuli by regulating mitochondrial membrane permeability (Morris et al., 2021). BDNF plays a neuroprotective role because of its neurotrophic, antiapoptotic and antioxidative properties and is able to increase the expression of SODs (Chen et al., 2017; Pemberton et al., 2021; Camuso et al., 2022). In our experiments, Ind significantly reduced *Bim*, *Fas-L* and *P27* upregulation and increased *Bcl-2* and *BDNF* downregulation induced by HFD. Taken together, these results suggest that Ind treatment can prevent neuronal apoptosis by modulating the expression of key apoptosis-related genes.

The relationships among neuronal apoptosis, oxidative damage, neuroinflammation and gut microbiota dysbiosis in the development of neural pathologies are well documented. Oxidative stress is one of the most important risk factors for neuronal apoptosis and can initiate neuroinflammatory responses mediated by microglia and astrocytes. Conversely, neuroinflammation can amplify oxidative damage and neuronal apoptosis, perpetuating a cycle of neurodegeneration (Shandilya et al., 2021). Moreover, dysbiosis of the gut microbiota can exacerbate neuroinflammation through various means, including increasing intestinal permeability and/or beneficial metabolite production, affecting neuronal health (Solanki et al., 2023).

Consequently, we considered the impact of Ind on the brain redox state and neuroinflammation triggered by HFD. In

agreement with previous studies (Moroz et al., 2008; Nuzzo et al., 2015, 2020; Terzo et al., 2023), we found that HFD increased malondialdehyde, RONS and NO levels, likely by downregulating the expression of the antioxidant enzyme SOD-2. Conversely, Ind supplementation prevented HFD-induced increases in oxidative stress markers and increased SOD-2 expression. These results, which are consistent with the antioxidative properties of the pigment betalain (Allegra et al., 2019; Attanzio et al., 2022; Terzo et al., 2021), provide evidence of the beneficial effects of Ind at the cerebral level in HFD-fed mice. We also verified the involvement of Nrf-2 in the protection of Ind against oxidative stress. Nrf-2 is a transcription factor that plays a significant role in the regulation of the cellular redox balance in neurons via genes encoding detoxifying and antioxidant enzymes (Hayes and Dinkova-Kostova, 2014). The observation that Nrf-2 nuclear accumulation was increased in the HFD + Ind brain suggests that Ind may facilitate Nrf-2 activation, leading to SOD-2 overexpression, which, in turn, reduces RONS and MDA. Therefore, activation of the Nrf-2/SOD-2 axis may be one of the mechanisms underlying the neuroprotective effects of Ind.

We found that Ind prevented the HFD-induced increase in the expression of some proinflammatory genes (*TNF-α* and *IL-6*) and proteins (iNOS and COX-2) in the brain. The expression of these proinflammatory mediators is tightly controlled by the activation of the redox-dependent transcription factor NF-B (Guo et al., 2024).

Interestingly, HFD induced NF-B activation. Therefore, it is possible to hypothesize that Ind is able to counteract HFD-induced neuroinflammation via the reduced activation of transcription factors, leading to decreases in downstream proinflammatory enzymes and gene expression.

To confirm the anti-inflammatory activity of Ind in the brain, we also evaluated the expression of GFAP, an astrocyte protein that is overexpressed in astrogliosis and inflammation (Jurga et al., 2021). The increase in HFD-induced gliosis and glial activation was markedly improved by Ind in superficial cortical sections. Moreover, since serum TNF-α, IL-1β and IL-6 can induce astrogliosis by crossing the blood–brain barrier, we evaluated the impact of Ind on plasma cytokine concentrations. Ind failed to affect the HFD-induced increase in TNF-α and IL-1β levels, suggesting that the beneficial effect on neuroinflammation is not mediated by an indirect action at the systemic level but rather by direct action in the brain. Indeed, unlike the majority of phytochemicals, Ind is able to cross the blood–brain barrier (Allegra et al., 2015).

Numerous studies have noted that the composition and metabolome of the gut microbiota are altered in various brain disorders, leading to the hypothesis that modulation of the gut microbiota may prevent or improve the development and progression of central nervous system pathologies (Rekha et al., 2024; Fung et al., 2017). In particular, evidence suggests that changes in the gut microbiota are involved in the neuroinflammation and cognitive impairment associated with obesity (Agustì et al., 2018; Zhang et al., 2019). Consequently, we analyzed the effects of Ind on the diversity and composition of the gut microbiota. Consistent with previous studies (Lee et al., 2019; Fang et al., 2021; Ye et al., 2021), HFD-fed mice presented decreased microbial diversity and formed a cluster that was distant from that of STD-fed mice. However, the microbial communities of Ind-treated mice clustered closely to those of HFD-fed mice, and the abundance of Ind-treated mice was similarly lower than that of STD-fed mice, suggesting that Ind failed to reverse HFD-induced gut dysbiosis. In addition, the *Firmicutes*/*Bacteroidetes* ratio, which is significantly increased in HFD-fed mice and is an indicator of obesity-linked microbial imbalance (Turnbaugh et al., 2006), was not modified by Ind supplementation. Interestingly, we detected decreases in the abundance of several minor phyla in HFD + ind mice: *Desulfobacterota*, *Proteobacteria* and *Deferribacterota*. In particular, the decrease in the abundance of *Proteobacteria*, the major source of LPS (Lin et al., 2020), could be beneficial because this phylum is associated with metabolic diseases, obesity and the development of AD (Hung et al., 2022).

Moreover, increases in *Desulfobacterota* and *Deferribacterota* have been associated with inflammatory damage, leading to alterations in energy metabolism (Gryaznova et al., 2022). Intriguingly, at the family level, Ind supplementation increased the abundance of *Lactobacillaceae* (*Lactobacillus* at the genus level and *Lactobacillus jhosonii* at the species level) and *Prevotellaceae* (*Alloprevotella* at the genus level), suggesting a shift toward a healthier microbial composition. In fact, *Lactobacillus* and *Alloprevotella* are considered probiotics with protective effects against dysfunctions of the intestinal barrier, inflammation and cognitive deficits (Wu et al., 2023; Zhang et al., 2023). In addition, these bacteria, as well as *Lachnospiraceae* and *Candidatus Saccharimonas*, which were increased in the HFD + Ind group, are known producers of SCFAs, primarily acetate, propionate and butyrate (De Filippo et al., 2010; Kong et al., 2019; Liu et al., 2019). SCFAs exert various beneficial effects because they improve the function of the intestinal barrier, preventing the translocation of harmful bacteria and toxins into the blood and promoting gut health (Saad et al., 2016). Additionally, SCFAs produced by gut bacteria play important roles in gut–brain communication (Silva et al., 2020). Once transported into the brain, they can modulate neuronal development and function (Rekha et al., 2024) and play anti-inflammatory and neuroprotective roles (Wang et al., 2018). Consequently, we determined SCFA levels in the plasma of the different animal groups. Surprisingly, in our experiments, we detected only acetate, whereas the concentrations of propionate and butyrate were under the revealing threshold. In any case, the levels of acetate, which were greatly decreased by HFD, were markedly increased by Ind, suggesting that acetate could mediate the beneficial impact of Ind in counteracting HFD-induced neuronal damage. Consistent with our hypothesis, a recent study demonstrated that acetate improves cognitive impairment and suppresses neuroinflammation in an AD mouse model by inhibiting the phosphorylation of NF-kβ and decreasing COX-2 and IL-1 expression (Liu et al., 2020).

Furthermore, Ind decreased the abundance of *Erysipelotrichaceae* and *Deferribacteraceae*, which are families that have the potential to induce inflammation (Liu et al., 2019) and are negatively correlated with SCFA-producing

bacteria (Do et al., 2023). Another positive modulator of the HFD microbiota by Ind consists of a reduction in the abundances of *Faecalibaculum Mucispirillum* and *Bilophila*, which are inflammation indicators associated with metabolic impairment (So et al., 2021; Yu et al., 2022). Finally, we found a significant reduction in *Blautia* abundance in HFD + Ind mice. Because *Blautia* has been linked to the development of glucose dysmetabolism, inflammation and diabetes (Kashtanova et al., 2018) as well as neurodegeneration (Keshavarzian et al., 2015; Voght et al., 2017), our observation fits well with the improvements induced by Ind in HFD-fed brains.

This study has several limitations that should be noted. Our results allow us to clarify whether the improvement in dysbiosis is the key mechanism by which Ind intake ameliorates neuronal damage. That changes in the gut microbiota are the main players responsible for the beneficial effects of Ind, we should examine the Ind impact in the absence of microbiota by using germ-free mice or animals treated with a cocktail of broad-spectrum antibiotics.

In conclusion, the present study shows, for the first time, the ability of Ind to combat HFD-induced neurodegeneration, brain oxidative stress and neuroinflammation. Modulation of redox-dependent NF-κB/Nrf2 activation and its downstream signaling axis appears to be a key mechanism underlying Ind-mediated neuroprotective effects. Importantly, phytochemical administration also positively modulates the composition and abundance of selected bacterial phyla, families, genera and species in the gut. Further experiments are necessary to clarify whether and how gut microbiota modulation is responsible for the neuroprotective effects of Ind.

Acknowledgments: *This work has received funding from the European Union -NextGenerationEU through the Italian Ministry of University and Research under PRIN PNRR REG D.R.1718-2022– Project number PRJ-1575 INDICA. The views and opinions expressed are those of the authors only and do not necessarily reflect those of the European Union or the European Commission. Neither the European Union nor the European Commission can be held responsible for them.*

Author contributions: *Conceptualization, TL; data curation: AA and MF; formal analysis: TS and AA; investigation: TS; methodology: CP, GM, ND, PP, PPA, AS, ICG, MA, RI, and AA; project administration: AM; resources: TL; supervision: AA and MF; writing – original draft: MF; writing – review & editing: TL and AM. All authors approved the final version of the paper.*

Conflicts of interest: *The authors declare that they have no conflicts of interest.*

Data availability statement: *All relevant data are within the paper and its Additional files.*

Additional files:

Additional Figure 1: *Flowchart of the study.*

Additional Figure 2: *Schematic diagram representing the timeline of the experimental protocol.*

References

Agustì A, García-Pardo MP, López-Almela I, Campillo I, Maes M, Romaní-Pérez M, Sanz Y (2018) Interplay between the gut-brain axis, obesity and cognitive function. Front Neurosci 12:155.

Allegra M, Ianaro A, Tersigni M, Panza E, Tesoriere L, Livrea MA (2014) Indicaxanthin from cactus pear fruit exerts an-ti-inflammatory effects in carrageenin-induced rat pleurisy. J Nutr 144:185-192.

Allegra M, Carletti F, Gambino G, Tutone M, Attanzio A, Tesoriere L, Ferraro G, Sardo P, Almerico AM, Livrea MA (2015) Indicaxanthin from Opuntia ficus-indica crosses the blood–brain barrier and modulates neuronal bioelectric activity in rat hippocampus at dietary-consistent amounts. J Agric Food Chem 63:7353-7360.

Allegra M, Tutone M, Tesoriere L, Almerico AM, Culletta G, Livrea MA, Attanzio A (2019) Indicaxanthin, a multitarget natural com-pound from Opuntia ficus-indica fruit: From its poly-pharmacological effects to biochemical mechanisms and molecular modelling studies. Eur J Med Chem 179:753-764.

Anjum I, Fayyaz M, Wajid A, Sohail W, Ali A (2018) Does obesity increase the risk of dementia: A literature review. Cureus 10:e2660.

Attanzio A, Frazzitta A, Busa' R, Tesoriere L, Livrea MA, Allegra M (2019) Indicaxanthin from Opuntia ficus indica (L. Mill) inhibits oxidized LDL-mediated human endothelial cell dysfunction through inhibition of NF-κB activation. Oxid Med Cell Longev 3457846.

Attanzio A, Restivo I, Tutone M, Tesoriere L, Allegra M, Livrea MA (2022) Redox properties, bioactivity and health effects of indicaxanthin, a bioavailable phytochemical from Opuntia ficus indica, L.: A critical review of accumulated evidence and perspectives. Antioxidants 11:2364.

Bustin SA, Benes V, Garson JA, Hellemans J, Huggett J, Kubista M, Mueller R, Nolan T, Pfaffl MW, Shipley GL, Vandesompele J, Wittwer CT (2009) The MIQE guidelines: minimum information for publication of quantitative real-time PCR experiments. Clin Chem 55:611-622.

Campisi A, Raciti G, Sposito G, Grasso R, Chiacchio MA, Spatuzza M, Attanzio A, Chiacchio U, Tesoriere L, Allegra M, Pellitteri R (2021) Amyloid-beta induces different expression pattern of tissue transglutaminase and its isoforms on olfactory ensheathing cells: modulatory effect of indicaxanthin. Int J Mol Sci 22:3388.

Camuso S, La Rosa P, Fiorenza MT, Canterini S (2022) Pleiotropic effects of BDNF on the cerebellum and hippocampus: Implications for neurodevelopmental disorders. Neurobiol Dis 163:105606.

Chen SD, Wu CL, Hwang WC, Yang DI (2017) More insight into BDNF against neurodegeneration: anti-apoptosis, anti-oxidation, and suppression of autophagy. Int J Mol Sci 18:545.

Chudoba C, Wardelmann K, Kleinridders A (2019) Molecular effects of dietary fatty acids on brain insulin action and mitochon-drial function. Biol Chem 400:991-1003.

De Filippo C, Cavalieri D, Di Paola M, Ramazzotti M, Poullet JB, Massart S, Collini S, Pieraccini G, Lionetti P (2010) Impact of diet in shaping gut microbiota revealed by a comparative study in children from Europe and rural Africa. Proc Natl Acad Sci U S A 107:14691-14696.

Dinel AL, André C, Aubert A, Ferreira G, Layé S, Castanon N (2011) Cognitive and emotional alterations are related to hippo-campal inflammation in a mouse model of metabolic syndrome. PLoS One 6:e24325.

Do MH, Lee HHL, Lee JE, Park M, Oh MJ, Lee HB, Park JH, Jhun H, Kim JH, Kang CH, Park HY (2023) Gellan gum prevents nonalcoholic fatty liver disease by modulating the gut microbiota and metabolites. Food Chem 400:134038.

Ethell DW, Buhler LA (2003) Fas ligand-mediated apoptosis in degenerative disorders of the brain. J Clin Immunol 23:363-70.

Fang D, Wang D, Ma G, Ji Y, Zheng H, Chen H, Zhaod M, Hua Q, Zhaoa L (2021) Auricularia polytricha noodles prevent hyperlipemia and modulate gut microbiota in high-fat diet fed mice. Food Sci Hum Wellness 10:431-441.

Fung TC, Olson CA, Hsiao EY (2017) Interactions between the microbiota, immune and nervous systems in health and disease. Nat Neurosci 20:145–55.

Galizzi G, Deidda I, Amato A, Calvi P, Terzo S, Caruana L, Scoglio S, Mulè F, Di Carlo M (2023) Aphanizomenon flos-aquae (AFA) Extract prevents neu-rodegeneration in the HFD mouse model by modulating astrocytes and microglia activation. Int J Mol Sci 24:4731.

Gryaznova M, Dvoretskaya Y, Burakova I, Syromyatnikov M, Popov E, Kokina A, Mikhaylov E, Popov V (2022) Dynamics of changes in the gut microbiota of healthy mice fed with lactic acid bacteria and bifidobacteria. Microorganisms 10:1020.

Guo Q, Jin Y, Chen X, Ye X, Shen X, Lin M, Zeng C, Zhou T, Zhang J (2024) NF-κB in biology and targeted therapy: new insights and translational implications. Signal Transduct Target Ther 9:53.

Habtemariam S (2018) Iridoids and other monoterpenes in the Alzheimer's brain: recent development and future prospects. Molecules 23:117.

Hayes JD, Dinkova-Kostova AT (2014) The Nrf2 regulatory network provides an interface between redox and intermediary metabolism. Trends Biochem Sci 39:199-218.

Hung CC, Chang CC, Huang CW, Nouchi R, Cheng CH (2022) Gut microbiota in patients with Alzheimer's disease spectrum: a systematic review and meta-analysis. Aging (Albany NY) 14:477-496.

Jaiswal S, Sharma P (2017) Role and regulation of p27 in neuronal apoptosis. J Neurochem 140:576-588.

Jardou M, Provost Q, Brossier C, Pinault E, Sauvage FL, Lawson R (2021) Alteration of the gut microbiome in mycopheno-late-induced enteropathy: impacts on the profile of short-chain fatty acids in a mouse model. BMC Pharmacol Toxicol 22:66.

Jurga AM, Paleczna M, Kadluczka J, Kuter KZ (2021) Beyond the GFAP-astrocyte protein markers in the brain. Biomolecules 11:1361.

Kashtanova DA, Tkacheva ON, Doudinskaya EN, Strazhesko ID, Kotovskaya YV, Popenko AS, Tyakht AV, Alexeev DG (2018) Gut microbiota in patients with different metabolic statuses: moscow study. Microorganisms 6:98.

Kempuraj D, Thangavel R, Natteru P, Selvakumar GP, Saeed D, Zahoor H, Zaheer S, Iyer SS, Zaheer A (2016) Neuroinflammation induces neurodegeneration. J Neurol Neurosurg Spine 1:1003.

Keshavarzian A, Green SJ, Engen PA, Voigt RM, Naqib A, Forsyth CB, Mutlu E, Shannon KM (2015) Colonic bacterial composition in Parkinson's disease. Mov Disord 30:1351-1360.

Kim DG, Krenz A, Toussaint LE, Maurer KJ, Robinson SA, Yan A, Torres L, Bynoe MS (2016) Nonalcoholic fatty liver disease induces signs of Alzheimer's disease (AD) in wildtype mice and accelerates pathological signs of AD in an AD model. J Neuroinflammation 13:1.

Kong C, Gao R, Yan X, Huang L, Qin H (2019) Probiotics improve gut microbiota dysbiosis in obese mice fed a high-fat or high-sucrose diet. Nutrition 60:175-184.

Lee PS, Teng CY, Hsieh KF, Chiou YS, Wu JC, Lu TJ, Pan MH (2019) Adzuki bean water extract attenuates obesity by modulating M2/M1 macrophage polarization and gut microbiota composition. Mol Nutr Food Res 63:e1900626.

Lin TL, Shu CC, Chen YM, Lu JJ, Wu TS, Lai WF, Tzeng CM, Lai HC, Lu CC (2020) Like cures like: pharmacological activity of anti-inflammatory lipopolysaccharides from gut microbiome. Front Pharmacol 11:554.

Liu J, Li H, Gong T, Chen W, Mao S, Kong Y, Yu J, Sun J (2020) Anti-neuroinflammatory effect of short-chain fatty acid acetate against Alzheimer's disease via upregulating GPR41 and inhibiting ERK/JNK/NF-kB. J Agric Food Chem 68:7152-7161.

Liu S, Qin P, Wang J (2019) High-fat diet alters the intestinal microbiota in streptozotocin-induced type 2 diabetic mice. Microorganisms 7:176.

Livingston G, et al. (2020) Dementia prevention, intervention, and care: 2020 report of the Lancet Commission. Lancet 396:413-446.

Maes ME, Schlamp CL, Nickells RW (2017) BAX to basics: how the BCL2 gene family controls the death of retinal ganglion cells. Prog Retin Eye Res 57:1-25.

Marseglia L, Manti S, D'Angelo G, Nicotera A, Parisi E, Di Rosa G, Gitto E, Arrigo T (2015) Oxidative stress in obesity: a critical component in human diseases. Intern J Mol Sci 16:378-400.

Miller AA, Spencer SJ (2014) Obesity and neuroinflammation: a pathway to cognitive impairment. Brain Behav Immun 42:10-21.

Moroz N, Tong M, Longato L, Xu H, de la Monte SM (2008) Limited Alzheimer-type neurodegeneration in experimental obesity and type 2 diabetes mellitus. J Alzheimers Dis 15:29-44.

Morris MCED, Bienias JL, Tangney CC, Wilson RS (2004) Dietary fat intake and 6-year cognitive change in an older biracial community population. Neurology 62:1573-1579.

Morris JL, Gillet G, Prudent J, Popgeorgiev N (2021) Bcl-2 family of proteins in the control of mitochondrial calcium signalling: an old chap with new roles. Int J Mol Sci 22:3730.

Noori T, Dehpour AR, Sureda A, Sobarzo-Sanchez E, Shirooie S (2021) Role of natural products for the treatment of Alzheimer's disease. Eur J Pharmacol 898:173974.

Nuzzo D, Picone P, Baldassano S, Caruana L, Messina E, Marino Gammazza A, Cappello F, Mulè F, Di Carlo M (2015) Insulin resistance as common molecular denominator linking obesity to Alzheimer's disease. Curr Alzheimer Res 12:723-35.

Nuzzo D, Galizzi G, Amato A, Terzo S, Picone P, Cristaldi L, Mulè F, Di Carlo M (2020) Regular intake of pistachio mitigates the deleterious effects of a high fat-diet in the brain of obese mice. Antioxidants 9:317.

O'Brien PD, Hinder LM, Callaghan BC, Feldman EL (2017) Neurological consequences of obesity. Lancet Neurol 16:465-477.

Pemberton JM, Pogmore JP, Andrews DW (2021) Neuronal cell life, death, and axonal degeneration as regulated by the BCL-2 family proteins. Cell Death Differ 28:108-122.

Picone P, Di Carlo M, Nuzzo D (2020) Obesity and Alzheimer's disease: molecular bases. Eur J Neurosci 52:3944-3950.

Pugazhenthi S, Qin L, Reddy PH (2017) Common neurodegenerative pathways in obesity, diabetes, and Alzheimer's disease. Biochim Biophys Acta Mol Basis Dis 1863:1037-1045.

Rahimi P, Abedimanesh S, Mesbah-Namin SA, Ostadrahimi A (2018) Betalains, the nature-inspired pigments, in health and diseases. Crit Rev Food Sci Nutr 30:1-30.

Rekha K, Venkidasamy B, Samynathan R, Nagella P, Rebezov M, Khayrullin M, Ponomarev E, Bouyahya A, Sarkar T, Shariati MA, Thiruvengadam M, Simal-Gandara J (2024) Short-chain fatty acid: An updated review on signaling, metabolism, and therapeutic effects. Crit Rev Food Sci Nutr 64:2461-2489.

Saad MJA, Santos A, Prada PO (2016) Linking gut microbiota and inflammation to obesity and insulin resistance. Physiology 31:283-293.

Shandilya S, Kumar S, Kumar Jha N, Kumar Kesari K, Ruokolainen J (2021) Interplay of gut microbiota and oxidative stress: Perspective on neurodegeneration and neuroprotection. J Adv Res 38:223-244.

Shi H, Yu Y, Lin D, Zheng P, Zhang P, Hu M, Wang Q, Pan W, Yang X, Hu T, Li Q, Tang R, Zhou F, Zheng K, Huang XF (2020) Beta-glucan attenuates cognitive impairment via the gut-brain axis in diet-induced obese mice. Microbiome 8:143.

Silva YP, Bernardi A, Frozza RL (2020) The role of short-chain fatty acids from gut microbiota in gut-brain communication. Front Endocrinol (Lausanne) 11:25.

Snowden SG, Ebshiana AA, Hye A, An Y, Pletnikova O, O'Brien R, Troncoso J, Legido-Quigley C, Thambisetty M (2017) Association between fatty acid metabolism in the brain and Alzheimer disease neuropathology and cognitive performance: a nontargeted metabolomics study. PLoS Med 14:e1002266.

So SY, Wu Q, Leung KS, Kundi ZM, Savidge TC, El-Nezami H (2021) Yeast β-glucan reduces obesity-associated Bilophila abundance and modulates bile acid metabolism in healthy and high-fat diet mouse models. Am J Physiol Gastrointest Liver Physiol 321:G639-655.

Solanki R, Karande A, Ranganathan P (2023) Emerging role of gut microbiota dysbiosis in neuroinflammation and neurodegeneration. Front Neurol 14:1149618.

Takahashi S, Tomita J, Nishioka K, Hisada T, Nishijima M (2014) Development of a prokaryotic universal primer for simultaneous analysis of Bacteria and Archaea using next-generation sequencing. PLoS One 9:e105592.

Terzo S, Attanzio A, Calvi P, Mulè F, Tesoriere L, Allegra M, Amato A (2021) Indicaxanthin from opuntia ficus-indica fruit ameliorates glucose dysmetabolism and counteracts insulin resistance in high-fat-diet-fed mice. Antioxidants (Basel) 11:80.

Terzo S, Calvi P, Nuzzo D, Picone P, Allegra M, Mulè F, Amato A (2023) Long-term ingestion of sicilian black bee chestnut honey and/or D-limonene counteracts brain damage induced by high fat-diet in obese mice. Int J Mol Sci 24:3467.

Tesoriere L, Allegra M., Butera D, Livrea MA (2004) Absorption, escretion and distribution in low density lipoproteins of dietary antioxidant betalains. Potential health effects of betalains in humans. Am J Clin Nutr 80:941-945.

Turnbaugh PJ, Ley RE, Mahowald MA, Magrini V, Mardis ER, Gordon JI (2006) An obesity-associated gut microbiome with increased capacity for energy harvest. Nature 444:1027-1031.

Valladolid-Acebes I, Stucchi P, Cano V, Fernández-Alfonso MS, Merino B, Gil-Ortega M, Fole A, Morales L, Ruiz-Gayo M, Del Olmo N (2011) High-fat diets impair spatial learning in the radial-arm maze in mice. Neurobiol Learn Mem 95:80-85.

Wang P, Zhang Y, Gong Y, Yang R, Chen Z, Hu W, Wu Y, Gao M, Xu X, Qin Y, Huang C (2018) Sodium butyrate triggers a functional elongation of microglial process via Akt-small RhoGTPase activation and HDACs inhibition. Neurobiol Dis 111:12-25.

Wang Y, Wang K, Yan J, Zhou Q, Wang X (2022) Recent progress in research on mechanisms of action of natural products against Alzheimer's disease: dietary plant polyphenols. Int J Mol Sci 23:13886.

Wanrooy BJ, Kumar KP, Wen SW, Qin CX, Ritchie RH, Wong CHY (2018) Distinct contributions of hyperglycemia and high-fat feeding in metabolic syndrome-induced neuroinflammation. J Neuroinflammation. 15:293.

World Health Organization (2021). World health statistics 2021: monitoring health for the SDGs, sustainable development goals. Available at: https://www.who.int/publications/i/item/9789240027053. Accessed July 18, 2023.

Wu Y, Niu X, Li P, Tong T, Wang Q, Zhang M, Li Y, Liu J, Li Z (2023) Lactobacillaceae improve cognitive dysfunction via regulating gut microbiota and suppressing Aβ deposits and neuroinflammation in APP/PS1 mice. Arch Microbiol 205:118.

Ye J, Zhao Y, Chen X, Zhou H, Yang Y, Zhang X, Huang Y, Zhang N, Lui EMK, Xiao M (2021) Puerh tea ameliorates obesity and modulates gut microbiota in high fat diet fed mice. Food Res Int 144:110360.

Yu Z, Yu XF, Kerem G, Ren PG (2022) Perturbation on gut microbiota impedes the onset of obesity in high fat diet-induced mice. Front Endocrinol (Lausanne) 13:795371.

Zhang P, Yu Y, Qin Y, Zhou Y, Tang R, Wang Q, Li X, Wang H, Weston-Green K, Huang XF, Zheng K (2019) Alterations to the microbiota-colon-brain axis in high-fat-diet-induced obese mice compared to diet-resistant mice. J Nutr Biochem 65:54-65.

Zhang S, Zeng L, Ma J, Xu W, Qu Y, Wang X, An X, Wang Q, Wu Y, Wang D, Chen H, Ai J (2023) Gut Prevotellaceae-GABAergic septohippocampal pathway mediates spatial memory impairment in high-fat diet-fed ovariectomized mice. Neurobiol Dis 177:105993.

C-Editors: Zhao M, Liu WJ; S-Editor: Li CH; L-Editors: Li CH, Song LP; T-Editor: Jia Y